JOURNAL OF MAGNETIC RESONANCE **132,** 255–259 (1998)
ARTICLE NO. MN981409

FT-EPR with a Nonresonant Probe: Use of a Truncated Coaxial Line

Kenneth A. Rubinson,*,[1] John A. Cook,† James B. Mitchell,† R. Murugesan,†
Murali C. Krishna,† and Sankaran Subramanian†

The Five Oaks Research Institute, 354 Oakwood Park Drive, Cincinnati, Ohio 45238-5157, and †Radiation Biology Section, National Cancer Institute, National Institutes of Health, Bethesda, Maryland 20892

Received March 11, 1997; revised January 13, 1998

A truncated transmission line probe (TLP) has been utilized to excite and detect time domain responses after pulsed excitation in electron paramagnetic resonance (EPR) spectroscopic experiments in the frequency range 200–400 MHz. The TLP device is a modified short-circuited coaxial line, which allows the irradiation of the sample by the traveling wave B_1 fields in the frequency range of kilohertz to 30 GHz. In EPR studies at 300 MHz carrier frequency, with 10 W incident power, a 45° pulse is 45 ns in duration. This corresponds to a 0.9-G B_1 field. Using the TLP, time-domain responses from the solid *N*-methyl pyridinium *tetra*-cyanoquinodimethane (TCNQ) were collected at 200, 250, 300, and 350 MHz, with the range limited by the amplifiers. In addition two tubes containing TCNQ placed side-by-side vertically along the axis of the probe were used to collect time domain responses in the presence of magnetic field gradients to test the feasibility of two-dimensional imaging using a TLP. The magnetic field gradient was steered in the *xz* plane and 36 projections were collected at 5° intervals. Using filtered back-projection image reconstruction, the two-dimensional spatial image in the *xz* plane was obtained at good resolution.

Key Words: **nonresonant; coaxial FT-EPR probe; magnetic resonance probes.**

INTRODUCTION

Nuclear magnetic resonance (NMR) studies generally have been conducted by placing the samples within various solenoidal or loop structures which form part of a tuned circuit. At the higher frequencies typical for electron paramagnetic resonance (EPR), samples are held in resonant cavities at a location of maximum B_1 field while centered at the node of the RF electric field standing wave. The resonant cavities are constructed with high *Q*-values to enhance signal-to-noise (*S*/*N*) for continuous wave (CW) EPR techniques. At X and K band, TE_{102}, TM_{011}, and loop-gap resonators are most common. However, matched, resonant coaxial quarter-wave lines have been used as sample cavities for low-frequency EPR since its early years (*1–8*).

In time-domain experiments, for the short T_2^* of most paramagnetic species, high-*Q* resonators possess excessive ringing times. Most commonly, this dead time has been decreased by lowering the *Q* of the resonators. However, the inherently low fill factors of the cavities limits the effectiveness of this strategy. At the opposite extreme is to eliminate the use of tuning/matching circuits, but this strategy is feasible only if the input RF power can be efficiently transformed to B_1 and the output efficiently picked up from the sample and relayed to the amplifier. To this end, the most common approach for broadband work has been to construct nonresonant solenoid delay lines. For instance, for NMR, Lowe and Engelsberg used a solenoid delay line with a relatively large bandwidth and short transient decay time (*9*). Delay-line coils have also been used in broadband EPR studies (*10, 11*). Most effective delay lines cannot have diameters more than about $\lambda/10$, and their small sizes at EPR frequencies have served to limit their use.

The TLPs, based on a short-circuited, coaxial line, can be used both with and without tune/match circuits. Without matching circuits, as for any shorted transmission line, the RF propagation is nearly frequency independent over NMR and EPR frequencies; the maximum B_1 field for all frequencies inherently resides at the sample's location at the short circuit. As such, the TLPs are expected to be effective for multiple frequency experiments. The bandwidth of a simple truncation is, however, not unlimited since the short circuit creates an antinode positions that can be at the detector, depending on the frequency. The bandwidth, then, depends on the acceptable level of power decrease, the frequency, the transmission line length to the detector, and the transmission line's loss properties. However, the bandwidths of the amplifiers are likely to be more restrictive.

In addition, no inherent ringdown time for the system is anticipated except for adventitious echoes associated with the bridge. Since probe ringing is an important factor in time-domain EPR spectroscopy, TLPs might be especially useful for such studies. This study describes the use of a TLP for time-domain EPR experiments in the frequency range 200–400 MHz.

EXPERIMENTAL

Probe Construction

Truncated line probes, similar to the one described here, were reported previously for CW-EPR (*12, 13*). Similar

[1] To whom correspondence should be addressed.

1090-7807/98 $25.00

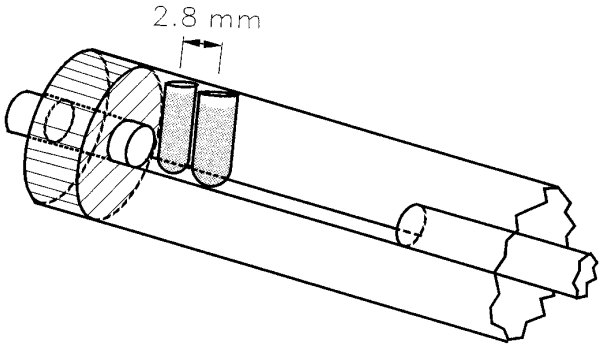

FIG. 1. Diagram of the TLP short circuited end and the placement of the TCNQ samples for imaging. Samples can also be placed along the axis and against the strip by insertion through a hole in the truncation.

probes, both untuned as well as tuned and matched, have been reported for use in NMR imaging (*14, 15*).

The truncated line is constructed of conventional cylindrical brass tubing (wall thickness 0.4 mm = 1/64 inch). The central conductor's diameter is 4.7 mm (3/16 inch), and the tube comprising the outer sheath has a 10.3-mm (13/32-inch) inner diameter. The short circuit is made using a cylindrical brass plug a few millimeters long that fits snugly between the coaxial conductors. The parts slide-fit together. The truncated line is attached to the RF source through a BNC connector (Amphenol #31-3376; Amphenol, Danbury, CT). The shield fits over the outside of the connector barrel, and the central conductor is soldered to the connector's central pin.

Access to the region inside the probe is allowed by cutting a 7 cm long, 180° sector out of the shield. The cutout is closed with a snugly fitting, movable cover in the form of a split cylinder 8 cm long, also made from brass tubing. For imaging, sample tubes were placed as shown in Fig. 1. For spectroscopy, tubes can be inserted and removed through a hole along the axis at the truncation without opening the cutout cover.

The B_1 field generated from the RF increases as the local current density increases. Thus, a significant RF magnetic field multiplication is achieved by removing most of the central conductor to leave only a conducting strip where the sample lies. In the probes used for this work, at least three-fourths of the conductor was removed. This is illustrated in Fig. 1. When one-fourth of the conductor remains, the local B_1 field is increased twofold (see Results).

Local impedances of the TLPs were measured using a time-domain reflectometer (TDR) (Tektronix Model 1502; Tektronix, Beaverton, OR). The impedance is calibrated relative to the 50-Ω cable connecting the probe to the TDR.

The period of a 180° pulse for ^{1}H-NMR of water in a capillary at ambient temperature was determined on a Philips 315 Imaging/Spectroscopy system with a 1.5-T magnet having a nominal proton frequency of 64 MHz. The time to the best null for a 180° pulse was found.

Samples

The paramagnetic samples used were powdered, solid TCNQ packed in tubes with O.D. 1.8 mm, I.D. 1.5 mm. Two short tubes were used for imaging, and a single, longer tube of sample inserted through the end was used for spectroscopy.

FT-EPR Instrument

The EPR instrument is a single-channel homebuilt machine operating between 200 and 400 MHz. The bandwidth limits are associated with the characteristics of the amplifiers. All the timings (pulse start, pulse stop, receiver gate, diplexer switch position) are generated by two Stanford Research Systems (Sunnyvale, CA 94089) DG535 Digital Delay Generators. All RF frequencies are derived from a Hewlett-Packard 8644A signal generator (Hewlett-Packard, San Jose, CA). The CW signal is gated by an RF switch to generate the transmitter pulse of appropriate width. The RF is amplified using an ENI Model 525LA 25 W linear amplifier (50 dB) and is applied to the TLP probe through a homemade transmit/receive (T/R) switch.

After a chosen delay (100 to 200 ns to blank switching transients) following the end of the RF pulse, the RF detection arm is connected to the TLP using the T/R switch. Then, the RF source is switched on to form the local oscillator to a mixer; applying the source to the mixer acts as a switch to allow the signal to continue to the data collection system. The magnitude of the local oscillator is set with an attenuator (Kay Model 839; Kay Elemetrics Corp., Pine Brook, NJ 07058).

The signals from the sample then are amplified with a 35-dB Miteq amplifier (Miteq Corp., Hauppauge, NY 11788) and further amplified with a homebuilt RF amplifier (19 dB). Another Kay attenuator is present between the amplifiers and set so that the second stage is not saturated. The resulting signal is then mixed with the RF carrier frequency and collected and summed. The data collection was done using a system based on an Analytek Model 2000RV2 ADC-averager (Tektronix, Beaverton, OR). The system has a nominal bandwidth of 1 GHz. For each FID or background (magnet off), 40,000 transients were averaged. Data collection times were approximately half a second.

Imaging was carried out with the same instrument in the presence of gradient magnetic fields provided by Helmholtz and Golay coils.

RESULTS

TLP Electrical Properties

The ratio of the diameter of the shield to the diameter of central conductor is 2.2, and the impedance of the TLP was found to be 48 ± 1 Ω along the entire 25-cm length except where the central conductor is cut out for the sample. There, the local impedance increases to about 60 Ω. The local impedance values were as expected since the impedance of a coaxial

conductor with air dielectric is 50 Ω when the ratio of the diameters of inner and outer surfaces is 2.30 (*16*).

Changing the frequency simply requires tuning the source to a new frequency and collecting data. No tuning of the probe was needed. As a result, a series of relaxation measurements at four different frequencies—for example, 200, 250, 300, and 350 MHz—were obtained in less than 15 min.

Probe Efficiency

The most straightforward figure of merit for the TLP is to determine the B_1 field generated for a given power. For an NMR experiment at 64 MHz, a ^{1}H 90° pulse was 195 μs long with 2.0 W (−34 dB relative to 5000 W) incident. The 195-μs 90° pulse translates to an average B_1 field of 0.3 G.

For the EPR results at 300 MHz, a 45° pulse was 45 ns long with 10 W incident power. This translates into a field of 0.9 G for the paramagnetic electrons. With the probe's flat response, the power must increase as the square of the B_1 increase. So we expect the fivefold increase in power between NMR and EPR to produce a 2.2-fold increase in B_1. The observed threefold increase in field is in moderate agreement indicating the consistency of the efficiency over the frequency range 64–400 MHz.

Calculation of the RF Field

We can approximate the RF magnetic field surrounding the central conductor of the coaxial line at a distance r from the cable axis using (*2, 13*)

$$B_\phi = \frac{I}{2\pi r}\,(\mathrm{A/m}). \qquad [1]$$

When 10 W power passes down the 48-Ω cable, a current of 0.46 A = (10 W/48 Ω)$^{1/2}$ is expected. The radius at the surface of the uncut inner conductor of the TLP is 2.35 mm, giving B_ϕ = 31 A/m. Since 1 A/m = $4\pi \times 10^{-3}$ G, Eq. [1] says to expect a field at the inner conductor's surface of 0.39 G. However, the reflection at the short circuit doubles the B_1 component compared to the traveling wave. Thus, 10 W incident is expected to produce an RF magnetic field of 0.78 G at the surface of the 2.35-mm-radius center conductor. With removal of three-fourths of the conductor, the field is expected to increase to approximately 1.6 G at the surface. The reason that the field only doubles rather than quadruples is that cutting the conductor open exposes the inner surface, so the conducting area is reduced to half that of the original, intact cylinder.

The final step in estimating the fields at the sample is to adjust for the sample's distance from the surface. The B_1 field decreases approximately as $1/r$ between the conductors, and the relative radius at the mid-distance between conductors is 1.6 times that at the surface of the central conductor. As a result, we expect a field of (1.6 G/1.6) = 1.0 G at the site between the conductors where the axis of the sample is situated. This simple, approximate model appears to provide moderate agreement with the 0.9 G measured from the EPR experiment.

Simple B-field modeling shows that B_1's are approximately equal on either side of the strip conductor. Experimentally, 90° pulses for ^{1}H NMR of water were the same within experimental error for samples placed on both sides, validating the modeling. These results suggest that either position may be used for a sample or, perhaps, both simultaneously for a sample and reference.

The location of the sample at the short circuit doubles the field compared to a transmission line, and cutting the central conductor to create a narrow strip at the short circuit increase the field approximately another factor of 2. As a result the unmatched line provides an increase in field equivalent to a Q of 16 before any further tune/match circuitry is added. Any increase in Q by a tune/match system augments that sensitivity but with a concomitant reduction in bandwidth. The benefits of this combination were demonstrated with a CW-TLP for low-field EPR reported earlier (*13*).

As the sample size is reduced, a still narrower strip can be used for the central conductor, allowing a further increase in B_1 field. With a thinner sample, the farthest distance of the cross-section lies closer to the conductor, enhancing the signal more since the material experiences a larger, more homogeneous B_1 field, and the reciprocal pickup of signals concomitantly increases.

Spectroscopy

In Fig. 2 are shown typical FIDs and spectra from a sample of solid TCNQ. In order to measure the resonance at difference frequencies, the oscillator was set, and the magnetic field adjusted to a few megahertz off resonance. Then, the FIDs were collected and averaged. The EPR data reduction consisted of subtracting the background from the signal. A subsequent Fourier transform provided the absorption spectra with their peaks at the offset frequency. The geometry was the same as used with a CW probe, with the sample inserted through a hole in the short-circuit end along the strip conductor (*13*).

Imaging

Shown in Fig. 3 are two views of an image of two TCNQ-filled tubes placed in the TLP with the geometry shown in Fig. 1. Larger samples will require higher power capabilities than are now available. We anticipate that images exterior to the probe will be able to be obtained as they were in NMR imaging (*14*), although the shielding of the system is not yet sufficient to do so.

CONCLUSIONS

The TLPs have a number of benefits, among which is the flexibility to allow a decrease in the width of the conducting region while keeping the B_1 field adequately homogeneous along the axis of the probe. The linear increases in the RF

field for the appropriate smaller samples may be far more beneficial than increasing the power quadratically. In addition, since the sample is enclosed within a closed shield, little RF leakage occurs either upon irradiation or in the power collection.

It is also worth noting that the RF magnetic field surrounds the central conductor of the coaxial line. This is a nearly ideal geometry for solenoid magnets, where the coaxial line is placed along the axis of the magnet. The B_1 field is then perpendicular to B_0 regardless of cylindrical angle. We can improve the homogeneity of the RF field by reshaping the conductors and truncation.

The impedance mismatch at the short circuit does cause some problems since the transmitter may need protection from the reflected pulse. However, the bandwidth is only limited by the locations of nodes at the location of the receiving amplifier.

A slight modification of the design of the TLP involving opening the outer conductor could have applications as a probe for detecting free radicals *in vivo* by EPR or FT-EPR. Such a probe has already been demonstrated in a number of sizes including a 2-mm catheter probe for ^{1}H MRI (*14*).

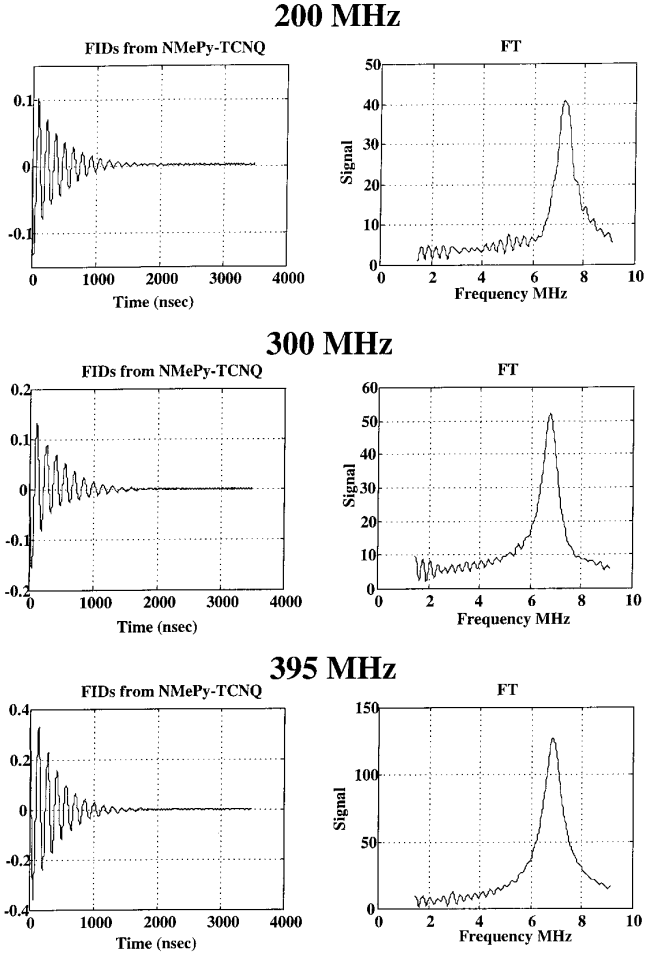

FIG. 2. FIDs and spectra of a TCNQ sample at three frequencies.

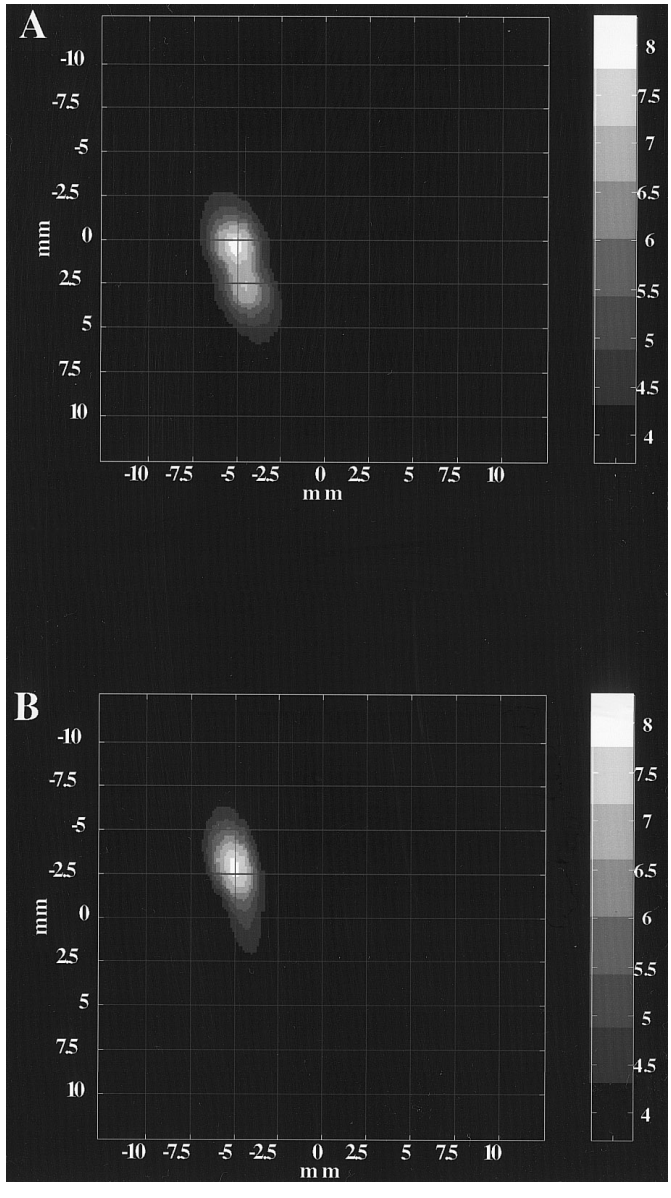

FIG. 3. Image of the TCNQ samples. (A) Cross section perpendicular to the sample tubes. (B) Slice through a tube. The curve at the bottom shows the shape of the tube. The intensity falloff at the top is due to the drop in B_1 radially from the central conductor.

ACKNOWLEDGMENTS

We thank Michael Pappas and David Krile of the Sensors Branch, Directorate of Avionics Engineering, Aeronautical Systems Division, Wright Patterson AFB, for hospitality. Also, David Krile and Clay White provided frequent technical help and insights. Frank Harrington of the Radiation Biology Branch NCI gave excellent machining assistance. We especially wish to thank Michael Boska who measured the NMR 90° pulses.

REFERENCES

1. J. Feher and A. F. Kip, *Phys. Rev.* **98,** 337–348 (1955).
2. M. S. Matheson and B. Smaller, *J. Chem. Phys.* **23,** 521–528 (1955).

3. R. S. Alger, T. H. Anderson, and L. A. Webb, *J. Chem. Phys.* **30,** 695–706 (1959).
4. R. F. Cook and L. G. Stoodley, *Intern. J. Rad. Biol.* **7,** 155–160 (1963).
5. W. Duncan and E. E. Schneider, *J. Sci. Instrum.* **42,** 395–398 (1965).
6. H. Grutzediek, K. D. Kramer, and W. Muller-Warmuth, *Rev. Sci. Instrum.* **36,** 1418 (1965).
7. M. J. Hill and S. J. Wyard, *J. Sci. Instrum.* **44,** 433–434 (1967).
8. W. Duncan, *J. Sci. Instrum.* **44,** 437–439 (1967).
9. I. J. Lowe and M. Engelsberg, *Rev. Sci. Instrum.* **45,** 631–639 (1974).
10. T. H. Wilmshurst, W. A. Gambling, and D. J. E. Ingram, *J. Electron. & Control (Int. J. Electron.)* **13,** 339–360 (1962).
11. C. P. Poole, ''Electron Spin Resonance: A Comprehensive Treatise on Experimental Techniques,'' 2nd ed., Wiley, New York (1983).
12. K. A. Rubinson, *Rev. Sci. Instrum.* **60,** 392–395 (1989).
13. K. A. Rubinson, J. Koscielniak, and L. J. Berliner, *J. Magn. Reson. A* **117,** 91–93 (1995).
14. K. A. Rubinson and M. Boska, *Magn. Reson. Imaging* **13,** 291–299 (1995).
15. K. A. Rubinson and M. Boska, *Magn. Reson. Imaging* **13,** 301–308 (1995).
16. S. Ramo, J. R. Whinnery, and T. van Duzer, ''Fields and Waves in Communication Electronics,'' 2nd. ed., Wiley, New York (1984).